HHS Public Access

Author manuscript

Alzheimers Dement. Author manuscript; available in PMC 2022 January 14.

Published in final edited form as:

Alzheimers Dement. 2021 December ; 17(12): 2020–2029. doi:10.1002/alz.12357.

Water Exchange Rate across the Blood-Brain Barrier is Associated with CSF Amyloid-β 42 in Healthy Older Adults

Brian T. Gold[1,4,5,*], **Xingfeng Shao**[6,*], **Tiffany L Sudduth**[4], **Gregory A. Jicha**[2,4], **Donna M. Wilcock**[3,4], **Elayna R. Seago**[1], **Danny JJ Wang**[6,7]

[1]Department of Neuroscience, College of Medicine, University of Kentucky, Lexington, KY 40536-0298 USA

[2]Department of Neurology, College of Medicine, University of Kentucky, Lexington, KY 40536-0298 USA

[3]Department of Physiology, College of Medicine, University of Kentucky, Lexington, KY 40536-0298 USA

[4]Sanders-Brown Center on Aging, College of Medicine, University of Kentucky, Lexington, KY 40536-0298 USA

[5]Magnetic Resonance Imaging and Spectroscopy Center, College of Medicine, University of Kentucky, Lexington, KY 40536-0298 USA

[6]Laboratory of FMRI Technology (LOFT), Mark & Mary Stevens Neuroimaging and Informatics Institute, Keck School of Medicine, University of Southern California

[7]Department of Neurology, Keck School of Medicine, University of Southern California

Abstract

Introduction: We tested if water exchange across the blood-brain-barrier (BBB), estimated with a noninvasive MRI technique, is associated with cerebrospinal fluid (CSF) biomarkers of Alzheimer's disease (AD) and neuropsychological function.

Methods: Forty cognitively normal older adults (67–86 years old) were scanned with diffusion-prepared, arterial spin labeling (DP-ASL) which estimates water exchange rate across the BBB (k_w). Participants also underwent CSF draw and neuropsychological testing. Multiple linear regression models were run with k_w as a predictor of CSF concentrations and neuropsychological scores.

Results: In multiple brain regions, BBB k_w was positively associated with CSF Aβ42 concentration levels. BBB k_w was only moderately associated with neuropsychological performance.

Discussion: Our results suggest that low water exchange rate across the BBB is associated with low CSF Aβ42 concentration. These findings suggest that k_w may be a promising noninvasive

Addresses for correspondence: Brian T. Gold, Ph.D. Department of Neuroscience, University of Kentucky College of Medicine, MN 364 Medical Sciences Building, 800 Rose Street, Lexington, KY, 40536-0298; Phone: 859-323-4813, brian.gold@uky.edu.

*Contributed equally to this work

indicator of BBB Aβ clearance functions, a possibility which should be further tested in future research.

Keywords

MRI; water exchange; BBB; biomarker; CSF; glymphatic

Background

Alzheimer's disease (AD) is the most common form of dementia, currently affecting more than 6 million Americans[1]. AD is characterized by progressive neuropathological changes that begin decades before the manifestation of cognitive and clinical declines[2,3]. Increasing evidence suggests that sporadic AD is associated with reduced amyloid-β (Aβ) clearance[4,5]. The blood-brain-barrier (BBB) is a key structure involved in Aβ clearance (via glymphatic and/or cerebrovascular function). The BBB consists of non-fenestrated vessels which tightly regulate the movement of ions and molecules between the blood and CNS[6,7]. The BBB serves to transport nutrients from the endothelial lumen and to protect the CNS from pathogens, toxins and inflammation among other functions[6,7].

Of particular relevance to AD, the BBB is involved in the clearance of interstitial solutes, including Aβ, from the brain[8,9]. A key BBB clearance pathway operates through a set of perivascular water channels (aquaporin-4; AQP4) at astrocytic endfeet. However, AQP4 channels are abnormally expressed in AD brains[10,11], which might potentially limit the clearance of Aβ[12,13,11]. For example, AQP4-deficient mice show significantly decreased water exchange rate, reflecting a potential delay in clearance of Aβ and other CNS solutes, compared to their wild-type counterparts[14].

Results from these postmortem human studies and animal models support a hypothesis that decreased water exchange rate across the BBB may be associated with reduced Aβ clearance in living humans. Testing this hypothesis requires a technique which can measure subtle alterations in water (and potentially solute) exchange rate across the BBB. The most commonly used MRI technique for assessment of BBB damage is dynamic contrast-enhanced (DCE) MRI. DCE-MRI can track paracellular leakage of gadolinium contrast as it passes between blood and brain (Ktrans), revealing important information about advanced tissue disruption. However, DCE-MRI may be less suited to assess more subtle forms of BBB dysfunction associated with alterations in active transport systems[9] although there may be DCE applications capable of assessing perfusion[15].

Recently, a noninvasive diffusion prepared arterial spin labeling (DP-ASL) MRI method has been validated for quantification of water exchange across the BBB[16–18]. The DP-ASL technique uses multiple diffusion weightings to differentiate magnetically tagged water signal from the capillary and brain parenchyma compartments based on a ~100-fold diffusion coefficient difference. The rate of water exchange (k_w) between these compartments is derived using a two-compartment model of the ASL signal with single-pass approximation (SPA)[17]. The k_w metric represents a ratio of capillary permeability surface area product of water (PSw) by capillary volume (Vc).

A recent validation study demonstrated that reduced k_w using this technique corresponds with both mannitol-induced BBB breakdown and histology in animal models[19]. DP-ASL k_w was also found to be correlated with DCE Ktrans in some brain regions[20]. The moderate correlations observed between DP-ASL k_w and DCE Ktrans may reflect overlapping yet different mechanisms assessed by these two metrics. The DCE and DP-ASL techniques also involve trade-offs. For example, DCE Ktrans provides higher spatial resolution. In contrast, DP-ASL likely provides a more sensitive marker of early-stage BBB dysfunction based on water exchange rate being about ~6000x faster than the exchange rate of gadolinium across the BBB[20]. DP-ASL also allows for computation of measures of cerebral perfusion such as cerebral blood flow (CBF) and arterial transit time (ATT), as assessed in the present study.

Here we sought to determine if water exchange rate across the BBB (k_w) is associated with cerebrospinal fluid (CSF) biomarkers of AD pathology (abeta42; Aβ42, total-tau; t-tau, hyperphosphorylated-tau; p-tau) in cognitively normal older adults. We hypothesized that k_w would be associated with CSF Aβ given that Aβ aggregates in interstitial fluid, and is thought to be cleared via BBB-related glymphatic mechanisms. In particular, we predicted that low k_w would be associated with low levels of CSF Aβ, which reflect high Aβ deposition in neuritic plaques[21,22]. A second, exploratory aim of the present study was to assess potential relationships between k_w and neuropsychological function. Specifically, we assessed if k_w was associated with performance on measures of episodic memory and executive function, cognitive domains of high relevance to preclinical AD.

Methods

Participants

Forty cognitively normal (CN) older adults were included in this study. One participant was excluded from analyses due to the presence of an old stroke within the right motor cortex that was not clinically evident by history at enrollment in the ADRC cohort. Summary group demographic characteristics of the 39 participants remaining participants (20 female, mean age=72.7) are shown in Table 1. All participants provided informed consent under a protocol approved by the Institutional Review Board of the University of Kentucky (UK). Participants were recruited from an existing longitudinal cohort of CN older adults at UK's Sanders-Brown Center on Aging (SBCoA)[23]. Exclusionary criteria for enrollment into the SBCoA cohort include major head injury, major psychiatric illness or current substance abuse, medical illnesses that are nonstable, impairing, or that have an effect on the CNS, chronic infectious diseases, major stroke, encephalitis, meningitis, or epilepsy[23].

Additional exclusion criteria for the present MRI study were claustrophobia, pacemakers, the presence of metal fragments or any metal implants that are incompatible with MRI. The majority of participants at UK's SBCoA agree to lumbar CSF draw. In the present MRI study, CN participants were recruited from the SBCoA on the basis of having available CSF data. A diagnosis of CN was established based on clinical consensus scores from the Uniform Data Set (UDS3) used by US Alzheimer's Disease Research Centers (ADRCs) [24] and a score of 26 or higher on the Mini-Mental State Exam (MMSE).

Imaging Protocol

Participants were scanned with a Siemens 3T PRISMA scanner, using a 64-channel head-coil, at UK's Magnetic Resonance Imaging and Spectroscopy Center. The following sequences were collected: a high resolution, multi-echo, T1-weighted anatomical image (MEMPR) and a 3D Gradient-and-Spin-Echo (GRASE) diffusion-prepared pCASL (DP-pCASL) sequence. The MEMPR sequence had four echoes [repetition time (TR)=2530ms; first echo time (TE1)=1.69ms echo time spacing (ΔTE)=1.86ms, flip angle (FA)=7°] and covered the entire brain [176 slices, field of view=256mm, parallel imaging (GRAPPA) factor=2, 1mm isotropic voxels, scan duration=5.53min].

The DP-pCASL sequence was performed with the following parameters: TR=4sec, TE=36.5ms, FOV=224mm, matrix size=64×64, 12 slices (10% oversampling), resolution=3.5×3.5×8mm^3, label/control duration=1500ms, centric ordering and optimized timing of background suppression for gray matter (GM) and white matter (WM) [25]. A two-stage approach was utilized to measure ATT and k_w: Fifteen repetitions were acquired during the flow encoding arterial spin tagging (FEAST) scan at post-labeling delay (PLD)=900ms and diffusion weighting (b-value) of 0 and 14 s/mm^2 with a total acquisition time of 4 minutes for estimating ATT[16]. The k_w metric was calculated from scans acquired at PLD=1800ms, when the labeled blood reaches the microvascular compartment, with b = 0 and 50 s/mm^2, respectively. Twenty repetitions were acquired for each b-value of the k_w scan, and the total acquisition time was 6 minutes. CBF was quantified from perfusion signals acquired at PLD=1800ms without diffusion preparation as described in detail elsewhere[18].

DP-ASL Analyses: TGV Regularized SPA Modeling for BBB Water Exchange Rate (k_w) Mapping

Control/label images were corrected for rigid head motion using SPM12 (Wellcome Trust Centre for Neuroimaging, UCL) and subtracted to obtain perfusion images. Temporal fluctuations were minimized using principal component analysis[26]. For DP-pCASL, the tissue and capillary compartments of the ASL signal were separated by a small diffusion gradient of 50 s/mm^2. The k_w map was calculated by a total-generalized-variation (TGV)[27] regularized SPA model[17] using the tissue (or capillary) fraction of the ASL signal at the PLD of 1800ms, incorporating ATT, T1 of arterial blood and brain tissue as inputs for the algorithm[18]. Arterial blood T1 was assumed to be 1.66 s, which is commonly used for CBF quantification[28]. Our simulation indicated that variations in arterial blood T1 (1.5s to 2.1s) led to <4% variations in k_w. A voxel-wise tissue T1 map was fitted from background suppressed control images acquired at 2 PLDs[26].The k_w, ATT and CBF maps, along with the M0 (T2 weighted structural image in the same space), were normalized to Montreal Neurological Institute (MNI) template space, and average values were measured in six regions of interests (ROIs) of relevance to AD: whole brain, frontal lobe, temporal lobe, parietal lobe, precuenus and medial temporal lobe (MTL; amygdala, hippocampus and parahippocampal gyrus). These ROIs were selected from the Anatomical Labeling Template in SPM, using participants' T1-weighted images, as described previously[29].

Cerebrospinal Fluid Collection and Analysis

CSF was drawn the morning after fasting since midnight according to current ADRC best practices/NIA guidelines. CSF lumbar draw was performed by a trained neurologist at the SBCoA (G.A.J) and then banked by the UK-ADRC Neuropathology Core. CSF was collected using a 20-gauge needle, 15ml sterile polypropylene collection tubes, and was stored in single use 0.5ml aliquots in polypropylene storage tubes at −80°C. CSF was analyzed using the Quanterix Simoa platform. $A\beta_{1–42}$ and phosphorylated-tau_{181} (p-tau_{181}) and total-tau (t-tau) were measured on the HD-1 instrument using the Neuro 3-plex A (Aβ40, Aβ42, total tau) assay at 1:200 and the pTau181 assay at 1:20 according to manufacturer's instructions. CSF samples were quantified in units of picograms per milliliter (pg/ml).

Neuropsychological Measures

The majority of participants underwent the UDS-3 neuropsychological battery and several additional measures administered to UK-ADRC participants. Composite measures of cognition were constructed for the AD-relevant domains of executive function and episodic memory. The executive function (EF) composite measure included the Trail Making Test Part A (TMT-A), Trail Making Test Part B (TMT-B) and the Digit Symbol test from the Wechsler Adult Intelligence Scale-IV (WAIS-DS). Scores on the TMT-A were regressed out of scores on the TMT-B and WAIS-DS in order to exclude components of raw processing and motor speed common to these tests (Salthouse, 2011). The resulting residuals were then combined to form a composite EF score by subtracting the TMT-B residuals (higher scores = worse performance) from the WAIS-DS residuals (higher scores = better performance) and dividing by 2. Therefore, higher EF composite scores reflected better performance. The episodic memory (MEM) composite included the CRAFT delayed recall and Benton Figure delayed recall. Total scores were divided by 2. Higher MEM composite scores reflected better performance.

Statistical Analyses

Statistical analyses were performed using SPSS 24 (IBM, Chicago, IL, USA). A series of multiple regression models were run to assess potential relationships between DP-ASL metrics with CSF biomarkers of AD and neuropsychological scores. Age and sex were included as covariates in all regression models. For the first set of analyses, separate multiple linear regression models were first run with DP-ASL metrics (k_w, CBF or ATT) as predictor variables of CSF biomarkers of AD (Aβ42, t-tau or p-tau). These initial regression models were statistically corrected for the 6 ROIs tested (p=0.05 / 6 ROIs; FWE, p=0.008). For the second set of analyses, separate multiple linear regression models were run to determine if k_w in any of those ROIs showing associations with CSF biomarkers of AD pathology (from the first set of regression models) were also associated with neuropsychological scores (EF or MEM composite scores). This second set of multiple linear regression analyses were statistically corrected for the 8 comparisons run (4 ROIs x 2 cognitive domains) (p=0.05 / 8; FWE, p=0.006).

For all regression models, assumptions of normality and heteroscedasticity of variance were explored by generating P-P plots, histograms and scatterplots of residuals. Evaluation of

these plots showed that our reported regression models met assumptions of normality and homoscedasticity. Multi-collinearity between predictors was explored using the variance inflation factor (VIF), with an upper limit of 5 implemented as a threshold value [30]. The VIF is reported for all models, with none exceeding a value of 1.5. Scatterplots of standardized residuals were created using participant z-scores values. Potential outliers in residual values were identified as being greater than 3 standard deviations from their group mean [31,32].

Results

The original data file and statistical results file are available as supplementary material. Summary group demographic and AD fluid biomarker characteristics of the 39 participants included in data analyses are shown in Table 1, with summary group DP-ASL values shown in Table 2.

Relationships between K_W and Fluid Biomarkers of AD Pathology

Relationships between k_w in ROIs (Figure 1) and fluid biomarkers of AD pathology were explored. Results (Table 3) indicated significant associations (FWE corrected p=0.008) between CSF Aβ42 concentration and k_w values in the whole brain (beta=0.51, t=3.4, p=0.002; VIF=1.04), frontal lobe (beta=0.50, t=3.4, p=0.002; VIF=1.04), parietal lobe (beta=0.56, t=3.9, p<0.001; VIF=1.03) and precuneus (beta=0.46, t=3.1, p=0.004; VIF=1.02), after controlling for age and sex (Figure 2, Panels A-D). The association between CSF Aβ42 concentration and k_w in the temporal lobe did not meet corrected significance (beta=0.42, t=2.6, p=0.015; VIF=1.11; Panel E). There was no relationship between CSF Aβ42 concentration and k_w in the MTL (beta= 0.21, t=1.2, p=0.236; VIF=1.13; Panel F). There were no significant associations between k_w in any of the ROIs and CSF t-tau concentration (P's ≥0.321) or between k_w in any of the ROIs and CSF p-tau concentration (P's ≥0.082).

Relationships between ATT, CBF and Fluid Biomarkers of AD Pathology

There were no significant associations (FWE corrected p=0.008) between ATT in any of the ROIs and Aβ42, p-tau or t-tau, although the relationship between ATT in the MTL and p-tau concentration level was significant at the uncorrected level (beta=−0.347, t=−2.1, p=0.042; VIF=1.10). There were no other associations between ATT in other regions and either p-tau or t-tau concentration levels (all P's ≥0.221). There were no associations between CBF in any of the ROIs and either Aβ42, p-tau or t-tau (all P's ≥0.121).

Relationships between kw and Neuropsychological Performance

Seven participants were missing neuropsychological data, leaving a total of 32 datasets for these analyses. To limit the number of comparisons, regression were only run for the 4 ROIs showing associations between k_w and CSF Aβ42 in the above models (whole brain, frontal lobe, parietal lobe and precuneus). Results (Table 4) indicated no significant associations (FWE corrected p = 0.006) between k_w in any of the 4 ROI and cognitive performance. At an uncorrected significance level, frontal lobe k_w was associated with MEM composite scores (beta=0.385, t=2.25, p=0.032; VIF=1.07; Figure 3, panel A), but not

with EF composite scores (beta=0.304, t=1.6 p=0.114; VIF=1.07). k_w in the other ROIs was not associated with MEM composite scores (all P's ≥0.292) or EF scores (all P's ≥0.342).

In summary, our results indicate that low k_w in multiple brain regions is associated with low CSF Aβ42 concentration. A schematic representation of the main pattern of kw-CSF Aβ42 results is illustrated in Figure 4. As can be seen in Figure 4, k_w values tend to track positively with CSF concentration scores while this pattern is less evident for CBF and ATT values.

Discussion

Our results provide evidence for an *in vivo* association between water exchange rate across the BBB (k_w) and CSF Aβ42 concentration. These findings suggest that k_w computed from a novel DP-pCASL sequence may be a potential indicator of BBB-related clearance functions. Implications of the k_w metric for cognitive functioning in healthy older adults remain less clear as k_w was only moderately associated with neuropsychological performance in our sample.

Associations of Kw, CBF and ATT with AD Fluid Biomarkers

Results indicated that low k_w in the whole brain, frontal lobe, parietal lobe and precuneus were each associated with low CSF Aβ42 concentration (reflecting high cerebral Aβ). In contrast, k_w was not associated with either CSF tau or p-tau in any ROI. The specificity of the link we observed between k_w in cortical regions and Aβ (as opposed to t-tau and/or p-tau) is in-keeping with findings that Aβ binding is more prominent in neocortex than MTL[33,34]. In addition, considering potential BBB-related clearance functions, Aβ aggregates extracellularly in the parenchyma, while tau accumulation is primarily an intracellular process unless the cell dies and release its proteinaceous components into the extracellular milieu[35]. Thus, our findings that k_w was more closely associated with CSF Aβ42 than tau appears consistent with expected role of BBB clearance functions during the preclinical (cognitively normal) stage.

Similarly, k_w was the only DP-pCASL metric associated with CSF Aβ42 concentration. Neither ATT nor CBF values were associated with CSF Aβ42 concentration. k_w values are a ratio of capillary permeability surface area product of water (PSw) by capillary volume (Vc). Lower k_w values can result from relatively low PSw or relatively high Vc values. The PSw is influenced by alterations in water channels. If water channel function is impaired or compromised, PSw would be decreased, and k_w values would be reduced. Further, as an extracellular protein, Aβ42 should be more closely linked with water exchange rate across the BBB than with measures of ATT or CBF, which are indices of cerebral perfusion. In keeping with this possibility, our results indicated that the k_w metric of water exchange across the BBB, but not perfusion, was associated with CSF Aβ.

The Potential Basis of k_w - Aβ42 Relationship

In late-onset sporadic AD, Aβ42 deposition appears more closely associated with impairment of Aβ efflux (clearance) than influx[5,36]. While direct exchange of water and CSF solutes such as Aβ may be mediated through BBB breakdown at the

neurovascular interface, it might also occur through the recently described glial lymphatic (glymphatic) pathway[37,38]. Whereas direct CNS-vascular permeability is mediated largely by inflammation, the glymphatic pathway is dependent on the AQP4 water channel, which selectively conducts water molecules across the BBB into the glymphatic pathways. In animal models, decreased AQP4 expression has been linked with reduced Aβ42 clearance from the brain[37,39] and deletion of the AQP4 gene results in increased Aβ plaque[40].

AQP4 water channels are typically localized to perivascular astrocytic endfeet that surround the cerebral vasculature[38,37] but are abnormally expressed in AD brains[10,11]. This includes both reduced localization of AQP4 to the cerebral vasculature[41] and reduced AQP4 expression in the vicinity of AB plaques. Reduced AQP4 expression may in turn contribute to reduced clearance and Aβ aggregation[42,13,42]. Thus, low k_w values from DP-ASL could in part reflect decreased localization or expression of AQP4 in individuals with higher cerebral Aβ concentration[41].

Associations of Kw and Cognitive Performance

We further sought to assess the associations of low water exchange rate across the BBB with cognitive performance. Results indicated that k_w was not associated with EF or MEM composite scores after controlling for multiple comparisons. Further, at an uncorrected statistical level, only the relationship between k_w in frontal cortex and MEM was significant. The weak relationship between k_w and neuropsychological function we observed could reflect limited sample size/power. In addition, k_w reductions in CN older adults may reflect early-stage BBB dysfunction which is not yet clinically significant. Future research should address k_w-cognitive relationships with larger sample sizes of adults who range in cognitive diagnosis from CN through impaired.

DP-pCASL as a Method for Quantifying Water Exchange across the BBB

Various methods have been proposed for quantifying water exchange rates including those using dynamic analysis of the first-pass signal of shutter-speed DCE-MRI[43], and with a novel multi-flip angle multi-echo (MFAME) scanning protocol[44]. Both methods require injection of contrast agents. As an alternative, ASL techniques use water as an endogenous tracer. Global water extraction rate and PSw can be measured with phase-contrast ASL (WEPCAST)[45]. Kinetic models have been proposed to map the regional water exchange rate using ASL sequences with signal preparation to separate intravascular and extravascular compartments based on the T2 difference[46,47,14] and the diffusion coefficient difference[48,49]. Considering that the pseudo-diffusion coefficient of capillary water is ~100-fold higher than that of the tissue[49], our proposed DP-pCASL method applies a small diffusion gradient so that two compartments of ASL signal can be reliably and efficiently separated and a whole brain k_w map can be obtained within 10 minutes.

Limitations

The k_w values reported in GM ROIs are likely to include some averaging of neighboring WM signal (i.e. partial volume effects) due to the relatively coarse voxel dimensions employed (3.5×3.5×8 mm3). In addition, the specific direction of k_w alterations (lower k_w versus higher k_w) in various neurological disorders requires further research. While

reduced BBB water exchange has been associated with aging and dementia[9], upregulation of AQP4 (and potentially increased k_w) has been reported in vascular disorders such as diabetes[50]. In our previous study, increased k_w was associated with increased vascular risk factors in Latinx participants[18]. The specific k_w alterations and underlying mechanisms related to AD and small vessel disease and other neurologic disorders await to be clarified in future studies. Further, it should be recognized that this is a cross-sectional study which is limited to a description of associations. Whether disruption of the glymphatic system or the direct cerebrovascular interface is responsible for the observed associations remains unclear. Future work investigating k_w in longitudinal datasets are important for answering these critical questions and driving the field forward. Such work should consider inclusion of PET-amyloid imaging for spatial localization not provided by CSF data.

Conclusions

The present results demonstrate that a non-invasive measure of water exchange rate across the BBB (k_w) is associated with lumbar CSF Aβ42 concentration levels. Our results suggest that k_w measured by a novel 3D GRASE DP-pCASL sequence shows promise as a non-invasive metric of BBB-related clearance in CN older adults. These findings need to be replicated in other cohorts, and in larger numbers of participants, in order to further evaluate the sensitivity and specificity of this non-invasive, potential marker of BBB-related clearance functions.

Supplementary Material

Refer to Web version on PubMed Central for supplementary material.

Acknowledgments

The authors thank Dr. Shoshana Bardach for help with participant recruitment and Beverly Meacham and Eric Foreman for assisting/conducting the MRI scans. This work was supported by the National Institutes of Health (grant numbers NIA R01AG055449, NIA P30 AG072946, NIGMS S10 OD023573, UH3-NS100614, R01-NS114382 and R01-EB028297). The content is solely the responsibility of the authors and does not necessarily represent the official views of these granting agencies. The authors declare no competing financial interests.

References

1. Brookmeyer R, Abdalla N, Kawas CH, Corrada MM. Forecasting the prevalence of preclinical and clinical Alzheimer's disease in the United States. Alzheimer's Dement. Published online 2018. doi:10.1016/j.jalz.2017.10.009
2. Resnick SM, Sojkova J, Zhou Y, et al. Longitudinal cognitive decline is associated with fibrillar amyloid-beta measured by [11C]PiB. Neurology. 2010;74(10):807–815. doi:10.1212/WNL.0b013e3181d3e3e9 [PubMed: 20147655]
3. Wilson RS, Leurgans SE, Boyle PA, Schneider JA, Bennett DA. Neurodegenerative basis of age-related cognitive decline. Neurology. 2010;75(12):1070–1078. doi:10.1212/WNL.0b013e3181f39adc [PubMed: 20844243]
4. Tarasoff-Conway JM, Carare RO, Osorio RS, et al. Imprimindo Extrato por Período. Nat Rev Neurol. 2015;11(8):457–470. doi:10.1038/nrneurol.2015.119.Clearance [PubMed: 26195256]
5. Wildsmith KR, Holley M, Savage JC, Skerrett R, Landreth GE. Wildsmith et al. (2013) Evidence for impaired amyloid β clearance in Alzheimer's disease.pdf. Published online 2013.
6. Zlokovic BV The Blood-Brain Barrier in Health and Chronic Neurodegenerative Disorders. Neuron. Published online 2008. doi:10.1016/j.neuron.2008.01.003

7. Daneman R The blood-brain barrier in health and disease. Ann Neurol. Published online 2012. doi:10.1002/ana.23648
8. Iliff JJ, Wang M, Liao Y, et al. A paravascular pathway facilitates CSF flow through the brain parenchyma and the clearance of interstitial solutes, including amyloid β. Sci Transl Med. 2012;4(147). doi:10.1126/scitranslmed.3003748
9. Dickie BR, Parker GJM, Parkes LM. Measuring water exchange across the blood-brain barrier using MRI. Prog Nucl Magn Reson Spectrosc. 2020;116:19–39. doi:10.1016/j.pnmrs.2019.09.002 [PubMed: 32130957]
10. Pérez E, Barrachina M, Rodríguez A, et al. Aquaporin expression in the cerebral cortex is increased at early stages of Alzheimer disease. Brain Res. 2007;1128(1):164–174. doi:10.1016/j.brainres.2006.09.109 [PubMed: 17123487]
11. Misawa T, Arima K, Mizusawa H, Satoh J ichi. Close association of water channel AQP1 with amyloid-β deposition in Alzheimer disease brains. Acta Neuropathol. 2008;116(3):247–260. doi:10.1007/s00401-008-0387-x [PubMed: 18509662]
12. Mestre H, Hablitz LM, Xavier ALR, et al. Aquaporin-4-dependent glymphatic solute transport in the rodent brain. Elife. 2018;7:1–31. doi:10.7554/eLife.40070
13. Zeppenfeld DM, Simon M, Haswell JD, et al. Association of perivascular localization of aquaporin-4 with cognition and Alzheimer disease in aging brains. JAMA Neurol. 2017;74(1):91–99. doi:10.1001/jamaneurol.2016.4370 [PubMed: 27893874]
14. Ohene Y, Harrison IF, Nahavandi P, et al. Non-invasive MRI of brain clearance pathways using multiple echo time arterial spin labelling: an aquaporin-4 study. Neuroimage. 2019;188(November 2018):515–523. doi:10.1016/j.neuroimage.2018.12.026 [PubMed: 30557661]
15. Larsson HBW, Courivaud F, Rostrup E, Hansen AE. Measurement of brain perfusion, blood volume, and blood-brain barrier permeability, using dynamic contrast-enhanced T1-weighted MRI at 3 tesla. Magn Reson Med. Published online 2009. doi:10.1002/mrm.22136
16. Wang J, Fernández-Seara MA, Wang S, St Lawrence KS. When perfusion meets diffusion: In vivo measurement of water permeability in human brain. J Cereb Blood Flow Metab. 2007;27(4):839–849. doi:10.1038/sj.jcbfm.9600398 [PubMed: 16969383]
17. St Lawrence KS, Owen D, Wang DJJ. A two-stage approach for measuring vascular water exchange and arterial transit time by diffusion-weighted perfusion MRI. Magn Reson Med. 2012;67(5):1275–1284. doi:10.1002/mrm.23104 [PubMed: 21858870]
18. Shao X, Ma SJ, Casey M, D'Orazio L, Ringman JM, Wang DJJ. Mapping water exchange across the blood-brain barrier using 3D diffusion-prepared arterial spin labeled perfusion MRI. Magn Reson Med. 2019;81(5):3065–3079. doi:10.1002/mrm.27632 [PubMed: 30561821]
19. Tiwari YV, Lu J, Shen Q, Cerqueira B, Duong TQ. Magnetic resonance imaging of blood–brain barrier permeability in ischemic stroke using diffusion-weighted arterial spin labeling in rats. J Cereb Blood Flow Metab. 2017;37(8):2706–2715. doi:10.1177/0271678X16673385 [PubMed: 27742887]
20. Shao X, Jann K, Ma SJ, et al. Comparison Between Blood-Brain Barrier Water Exchange Rate and Permeability to Gadolinium-Based Contrast Agent in an Elderly Cohort. Front Neurosci. Published online 2020. doi:10.3389/fnins.2020.571480
21. Blennow K, Mattsson N, Schöll M, Hansson O, Zetterberg H. Amyloid biomarkers in Alzheimer's disease. Trends Pharmacol Sci. Published online 2015. doi:10.1016/j.tips.2015.03.002
22. Klunk WE, Engler H, Nordberg A, et al. Imaging Brain Amyloid in Alzheimer's Disease with Pittsburgh Compound-B. Ann Neurol. Published online 2004. doi:10.1002/ana.20009
23. Schmitt FA, Nelson PT, Abner E, et al. University of Kentucky Sanders-Brown Healthy Brain Aging Volunteers: Donor Characteristics, Procedures and Neuropathology. Curr Alzheimer Res. 2012;9(6):724–733. doi:10.2174/156720512801322591 [PubMed: 22471862]
24. Besser L, Kukull W, Knopman DS, et al. Version 3 of the national Alzheimer's coordinating center's uniform data set. Alzheimer Dis Assoc Disord. Published online 2018. doi:10.1097/WAD.0000000000000279
25. Shao X, Wang Y, Moeller S, Wang DJJ. A constrained slice-dependent background suppression scheme for simultaneous multislice pseudo-continuous arterial spin labeling. Magn Reson Med. 2018;79(1):394–400. doi:10.1002/mrm.26643 [PubMed: 28198576]

26. Shao X, Tisdall MD, Wang DJ, van der Kouwe AJW. Prospective motion correction for 3D GRASE pCASL with volumetric navigators. Proc Int Soc Magn Reson Med Sci Meet Exhib Int Soc Magn Reson Med Sci Meet Exhib. Published online 2017.
27. Spann SM, Shao X, Wang DJ, et al. Robust single-shot acquisition of high resolution whole brain ASL images by combining time-dependent 2D CAPIRINHA sampling with spatio-temporal TGV reconstruction. Neuroimage. Published online 2020. doi:10.1016/j.neuroimage.2019.116337
28. Lu H, Clingman C, Golay X, Van Zijl PCM. Determining the longitudinal relaxation time (T1) of blood at 3.0 tesla. Magn Reson Med. Published online 2004. doi:10.1002/mrm.20178
29. Yan L, Liu CY, Wong KP, et al. Regional association of pCASL-MRI with FDG-PET and PiB-PET in people at risk for autosomal dominant Alzheimer's disease. NeuroImage Clin. 2018;17(November 2017):751–760. doi:10.1016/j.nicl.2017.12.003 [PubMed: 29527482]
30. Stine RA. Graphical interpretation of variance inflation factors. Am Stat. Published online 1995. doi:10.1080/00031305.1995.10476113
31. B V, L. T Outliers in Statistical Data, 3rd Edition. J. Wiley and Sons; 1994.
32. J CM, M GH, R CS. Data Analysis: A Model Comparison Approach, 2nd Edition. Routledge; 2009.
33. Braak H, Braak E. Neuropathological stageing of Alzheimer-related changes. Acta Neuropathol. Published online 1991. doi:10.1007/BF00308809
34. T DR, R U, O M, B. H Phases of Aβ-deposition in the human brain and its relevance for the development of AD. Neurology. Published online 2002.
35. Binder LI, Frankfurter A, Rebhun LI. The Distribution Central Nervous of Tau in System the Mammalian. J Cell Biol. Published online 1985. doi:10.1083/jcb.101.4.1371
36. Tarasoff-Conway JM, Carare RO, Osorio RS, et al. Clearance systems in the brain - Implications for Alzheimer disease. Nat Rev Neurol. Published online 2015. doi:10.1038/nrneurol.2015.119
37. Iliff JJ, Wang M, Liao Y, et al. A paravascular pathway facilitates CSF flow through the brain parenchyma and the clearance of interstitial solutes, including amyloid β. Sci Transl Med. 2012;4(147). doi:10.1126/scitranslmed.3003748
38. Iliff JJ, Lee H, Yu M, et al. Brain-wide pathway for waste clearance captured by contrast-enhanced MRI. J Clin Invest. 2013;123(3):1299–1309. doi:10.1172/JCI67677 [PubMed: 23434588]
39. Shibata M, Yamada S, Ram Kumar S, et al. Clearance of Alzheimer's amyloid-β1–40 peptide from brain by LDL receptor-related protein-1 at the blood-brain barrier. J Clin Invest. Published online 2000. doi:10.1172/JCI10498
40. Xu Z, Xiao N, Chen Y, et al. Deletion of aquaporin-4 in APP/PS1 mice exacerbates brain Aβ accumulation and memory deficits. Mol Neurodegener. 2015;10(1):1–16. doi:10.1186/s13024-015-0056-1 [PubMed: 25567526]
41. Wilcock DM, Vitek MP, Colton CA. Vascular amyloid alters astrocytic water and potassium channels in mouse models and humans with Alzheimer's disease. Neuroscience. 2009;159(3):1055–1069. doi:10.1016/j.neuroscience.2009.01.023 [PubMed: 19356689]
42. Hoshi A, Yamamoto T, Shimizu K, et al. Characteristics of aquaporin expression surrounding senile plaques and cerebral amyloid angiopathy in Alzheimer disease. J Neuropathol Exp Neurol. 2012;71(8):750–759. doi:10.1097/NEN.0b013e3182632566 [PubMed: 22805778]
43. Rooney WD, Li X, Sammi MK, Bourdette DN, Neuwelt EA, Springer CS. Mapping human brain capillary water lifetime: High-resolution metabolic neuroimaging. NMR Biomed. Published online 2015. doi:10.1002/nbm.3294
44. Dickie BR, Vandesquille M, Ulloa J, Boutin H, Parkes LM, Parker GJM. Water-exchange MRI detects subtle blood-brain barrier breakdown in Alzheimer's disease rats. Neuroimage. Published online 2019. doi:10.1016/j.neuroimage.2018.09.030
45. Lin Z, Li Y, Su P, et al. Non-contrast MR imaging of blood-brain barrier permeability to water. Magn Reson Med. Published online 2018. doi:10.1002/mrm.27141
46. Wells JA, Siow B, Lythgoe MF, Thomas DL. Measuring biexponential transverse relaxation of the ASL signal at 9.4 T to estimate arterial oxygen saturation and the time of exchange of labeled blood water into cortical brain tissue. J Cereb Blood Flow Metab. 2013;33(2):215–224. doi:10.1038/jcbfm.2012.156 [PubMed: 23168531]

47. Gregori J, Schuff N, Kern R, Günther M. T2-based arterial spin labeling measurements of blood to tissue water transfer in human brain. J Magn Reson Imaging. Published online 2013. doi:10.1002/jmri.23822

48. Wengler K, Bangiyev L, Canli T, Duong TQ, Schweitzer ME, He X. 3D MRI of whole-brain water permeability with intrinsic diffusivity encoding of arterial labeled spin (IDEALS). Neuroimage. Published online 2019. doi:10.1016/j.neuroimage.2019.01.035

49. Shao X, Ma SJ, Casey M, D'Orazio L, Ringman JM, Wang DJJ. Mapping water exchange across the blood–brain barrier using 3D diffusion-prepared arterial spin labeled perfusion MRI. Magn Reson Med. Published online 2019. doi:10.1002/mrm.27632

50. Plog BA, Nedergaard M. The Glymphatic System in Central Nervous System Health and Disease: Past, Present, and Future. Annu Rev Pathol Mech Dis. Published online 2018. doi:10.1146/annurev-pathol-051217-111018

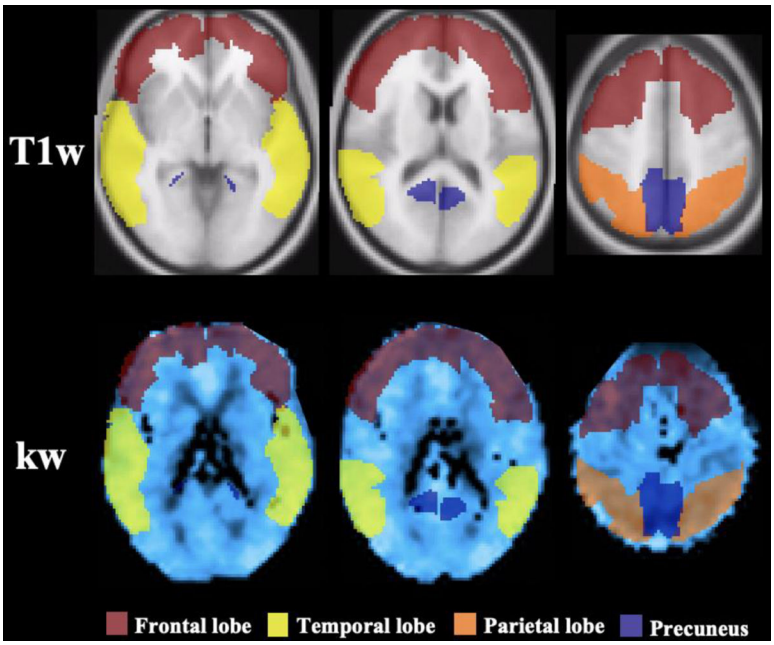

Figure 1.

Sample ROIs. Representations of masks used to extract values from the frontal lobe (maroon), temporal lobe (yellow), parietal lobe (orange) and precuneus (blue). ROIs are presented on a T1-weighted image (first row) and on a representative participant's k_w map in normalized space (second row). Columns from left-to-right show horizontal slices moving in the inferior-to-superior direction. The same ROI masks were used for extraction of ATT and CBF values.

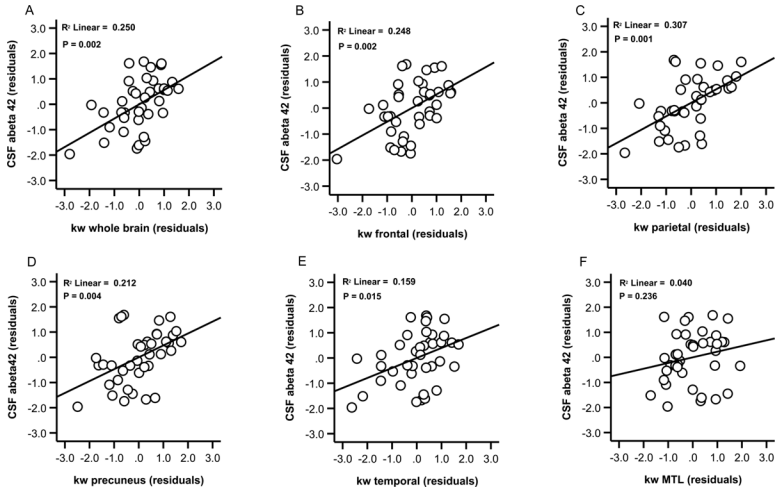

Figure 2.

Relationships between k_w values and CSF Aβ42 concentration. Scatter plots show k_w values in the whole brain (A), frontal lobe (B), parietal lobe (C) precuneus (D), temporal lobe (E) and MTL (F) plotted against CSF Aβ42 concentration. Plots show residual associations after controlling for age and sex.

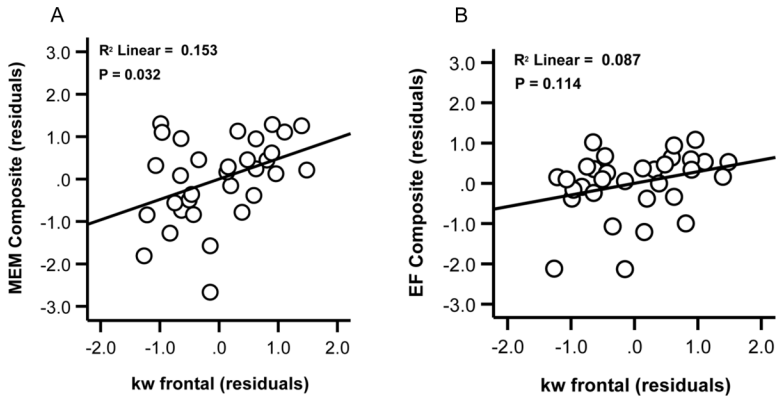

Figure 3.

Relations between k_W in the frontal lobe and neuropsychological scores. Scatter plots show k_W values in the frontal lobe against MEM composite scores, (A) and against EF composite scores, after controlling for age and sex (B).

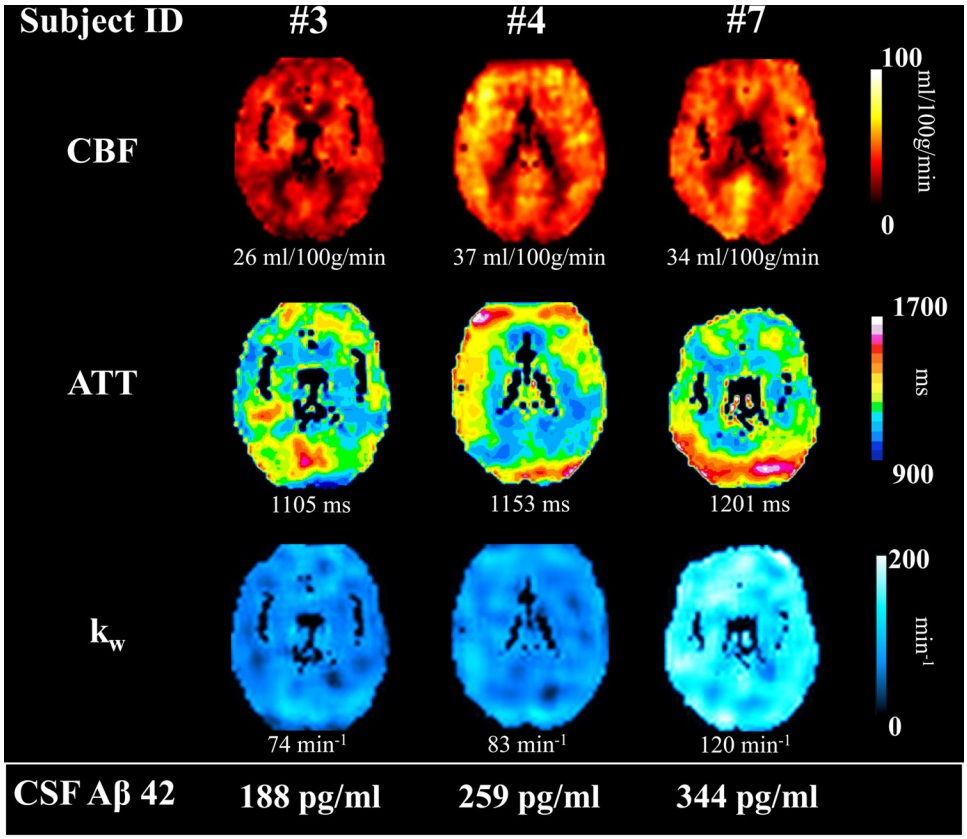

Figure 4.

Schematic representation of findings. Maps of CBF, ATT and k_w are presented from three representative participants showing the trend of increasing k_w values being associated with increasing CSF Aβ42 concentration (from left to right). Participants' whole brain CBF, ATT and k_w values are presented below their maps. Participants' CSF Aβ42 concentration values are presented at the bottom of the figure, within the white box.

Table 1.

Mean Group Demographic Values and CSF AD Biomarker Values

N	**39**
Age (Years)	72.7 [67–86]
Sex (F/M)	20/19
Education (Years)	16.64 (2.26)
MMSE	28.90 (1.43)
Aβ42 (pg/ml)	294.85 (76.13)
T-tau	62.74 (26.82)
P-tau	23.23 (16.46)

Notes: The table lists the total number of participants, mean and range for age, male/female distribution and mean and standard deviation (SD) for years of education, MMSE, Aβ42, t-tau and p-tau (pg/ml).

Table 2.

Mean Group Values for DP-ASL Metrics of k_w, ATT and CBF

	k_w	ATT	CBF
Whole Brain	98.27 (19.77)	1223.01 (101.65)	32.17 (9.02)
Frontal Lobe	104.42 (22.18)	1232.48 (115.90)	31.74 (9.65)
Temporal Lobe	94.76 (26.06)	1167.48 (116.63)	32.97 (9.94)
Parietal Lobe	83.21 (28.34)	1353.37 (148.20)	31.24 (11.54)
Precuneus	85.96 (28.79)	1334.03 (159.04)	33.24 (10.89)
Medial Temporal Lobe	85.87 (27.32)	942.38 (223.70)	22.88 (8.76)

Notes: The table lists mean and standard deviation (SD) in each ROI for the metrics of k_W, ATT and CBF.

Table 3.

Relationships between k_w and Fluid Biomarkers of AD pathology

	CSF Aβ42		CSF T-Tau		CSF P-Tau	
BBB Water Exchange (k_w)	**Beta-Value**	**P-Value**	**Beta-Value**	**P-Value**	**Beta-Value**	**P-Value**
Whole Brain	0.51	0.002	0.09	0.549	−0.24	0.167
Frontal Lobe	0.50	0.002	0.01	0.999	−0.18	0.287
Parietal Lobe	0.56	< 0.001	0.12	0.423	−0.29	0.082
Temporal Lobe	0.42	0.015	0.16	0.321	−0.21	0.244
Precuneus	0.46	0.004	0.03	0.822	−0.24	0.150
Medial Temporal Lobe	0.21	0.236	0.12	0.464	−0.265	0.132

Table 4.

Relationships between k_w and Neuropsychological Scores

	Episodic Memory		Executive Function	
BBB Water Exchange (k_w)	**Beta-Value**	**P-Value**	**Beta-Value**	**P-Value**
Whole Brain	0.19	0.292	0.19	0.342
Frontal Lobe	0.385	0.032	0.304	0.114
Parietal Lobe	0.18	0.322	0.02	0.925
Precuneus	0.09	0.632	0.12	0.528